9-14-2015

Far From 'Easy' Spectroscopy with the 8π and GRIFFIN Spectrometers at TRIUMF-ISAC

Steven W. Yates
University of Kentucky, yates@uky.edu

P. E. Garrett
University of Guelph, Canada

A. J. Radich
University of Guelph, Canada

J. M. Allmond
Oak Ridge National Laboratory

C. Andreoiu
Simon Fraser University, Canada

See next page for additional authors

Far From 'Easy' Spectroscopy with the 8π and GRIFFIN Spectrometers at TRIUMF-ISAC

P.E. Garrett[1], A.J. Radich[1], J.M. Allmond[2], C. Andreoiu[3], G.C. Ball[4], P.C. Bender[4,11], L. Bianco[1,12], V. Bildstein[1], H. Bidaman[1], R. Braid[5], C. Burbadge[1], S. Chagnon-Lessard[1,13], D.S. Cross[3], G. Deng[1], G.A Demand[1], A. Diaz Varela[1], M.R. Dunlop[1], R. Dunlop[1], P. Finlay[1,14], A.B. Garnsworthy[4], G.F. Grinyer[1,15], G. Hackman[4], B. Hadinia[1], S. Ilyushkin[5], B. Jigmeddorj[1], D. Kisliuk[1], K. Kuhn[5], A.T. Laffoley[1], K.G. Leach[1,3,4], A.D. MacLean[1], J. Michetti-Wilson[1], D. Miller[4], W. Moore[5], B. Olaizola[1], J.N. Orce[4,6], C.J. Pearson[4], J.L. Pore[3], M.M. Rajabali[4,16], E.T. Rand[1], F. Sarazin[5], J.K. Smith[4], K. Starosta[3], C.S. Sumithrarachchi[1,11], C.E. Svensson[1], S. Triambak[4,6,7], J. Turko[1], Z.M. Wang[3,4], J.L. Wood[8], J. Wong[1], S.J. Williams[4,11], S.W. Yates[9], E.F. Zganjar[10]

[1] Department of Physics, University of Guelph, Guelph, ON, N1G2W1, Canada
[2] Physics Division, Oak Ridge National Laboratory, Oak Ridge, TN 37831, USA
[3] Department of Chemistry, Simon Fraser University, Burnaby, BC, V5A1S6, Canada
[4] TRIUMF, 4004 Wesbrook Mall, Vancouver, BC, V6T 2A3, Canada
[5] Department of Physics, Colorado School of Mines, Golden, CO 80401, USA
[6] Department of Physics, University of the Western Cape, P/B X17, Bellville ZA-7535, South Africa
[7] iThemba LABS, P.O. Box 722, Somerset West 7129, South Africa
[8] School of Physics, Georgia Institute of Technology, Atlanta, GA 30332-0430, USA
[9] Departments of Chemistry and Physics & Astronomy, University of Kentucky, Lexington, KY 40506-0055, USA
[10] Department of Physics & Astronomy, Louisiana State University, Baton Rouge, LA 70803, USA

E-mail: pgarrett@physics.uoguelph.ca

Abstract.
The 8π spectrometer, installed at the TRIUMF-ISAC facility, was the world's most sensitive γ-ray spectrometer dedicated to β-decay studies. A description is given of the 8π spectrometer

[11] Present address: National Superconducting Cyclotron Laboratory, Michigan State University, East Lansing, MI 48824, USA
[12] Present address: DESY Photon Science, Notkestrasse 85 D-22607 Hamburg, Germany
[13] Present address: Department of Physics, University of Ottawa, 150 Louis-Pasteur, Ottawa, ON K1N 6N5, Canada
[14] Present address: Instituut voor Kern-en Stralingsfysica, K.U. Leuven, Celestijnenlaan 200D, B-3001 Leuven, Belgium
[15] Present address: Grand Accélérateur National d'Ions Lourds (GANIL), CEA/DSM-CNRS/IN2P3, Bvd Henri Becquerel, 14076 Caen, France
[16] Present address: Department of Physics, Tennessee Technological University, Cookeville, TN 38505, USA

and its auxiliary detectors including the plastic scintillator array SCEPTAR used for β-particle tagging and the Si(Li) array PACES for conversion electron measurements, its moving tape collector, and its data acquisition system. The recent investigation of the decay of ^{124}Cs to study the nuclear structure of ^{124}Xe, and how the β-decay measurements complemented previous Coulomb excitation studies, is highlighted, including the extraction of the deformation parameters for the excited 0^+ bands in ^{124}Xe. As a by-product, the decay scheme of the (7^+) ^{124}Cs isomeric state, for which the data from the PACES detectors were vital, was studied. Finally, a description of the new GRIFFIN spectrometer, which uses the same auxiliary detectors as the 8π spectrometer, is given.

1. Introduction

The programme of γ-ray spectroscopy following β-decay at TRIUMF-ISAC is pursued along three main themes: high-precision measurements of nuclei for tests of the Standard Model, mainly associated with Fermi super-allowed β^+ emitters; studies of nuclei near stability emphasizing high-statistics for both γ-γ and γ-e^- coincidences to test the nature of excited states, especially collective states; and studies of nuclei far from stability to elucidate the evolution of structure at the extremes of N/Z ratios. Until the end of 2013, the main tool for the γ-ray spectroscopy programme was the 8π spectrometer [1, 2] – a second-generation γ-ray detector array that was designed and built in the early-to-mid 1980s for high-spin studies at the Chalk River Laboratories. In January 2014, the 8π spectrometer was decommissioned at TRIUMF-ISAC to make way for the new GRIFFIN spectrometer [3]. GRIFFIN, a state-of-the-art HPGe clover-detector array, represents a substantial leap forward in both detection efficiency and data through-put, and will be transformative in its ability to enable high-statistics measurements and studies of nuclei far from stability. The 8π spectrometer will be re-commissioned at Simon Fraser University where it will be used in experiments involving fission with fast neutrons.

In the current contribution, the 8π spectrometer is described in some detail and selected recent results obtained will be outlined, concentrating mainly on the spectroscopy of ^{124}Xe following the decay of ^{124}Cs, as well as the elucidation of the decay scheme of the ^{124}Cs^m isomeric state, that highlight some of the capabilities of the 8π spectrometer and its auxiliary detectors. This

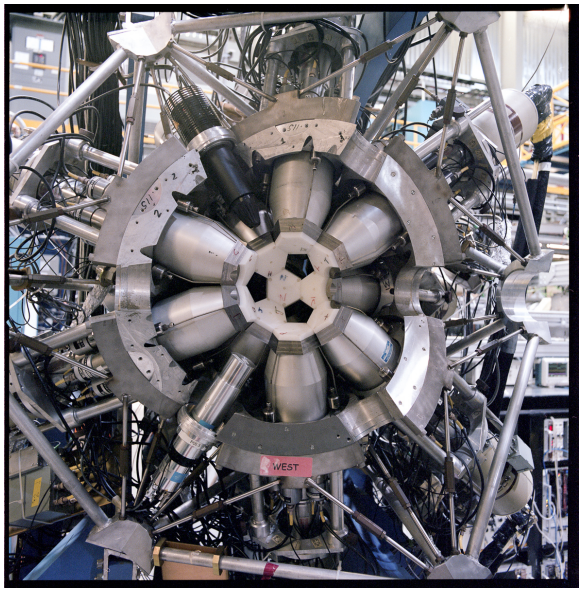

Figure 1. Photograph of one hemisphere of the 8π spectrometer. Clearly visible are 6 of the BGO Compton-suppression shields. Attached over the inner-facing end of the BGO shields are densalloy collimators that attenuate the radiation from the source from entering the BGO detectors. On the inner surface is delrin shielding designed to largely prevent the high-energy β particles from entering the Ge detectors while minimising the amount of hard bremsstrahlung radiation. Also visible are auxiliary detectors used for timing purposes placed in two of the available pentagonal openings; on the upper left (in black) is a BaF_2 detector with its photo-multiplier tube (PMT), and the lower left a $LaBr_3$ detector and its PMT.

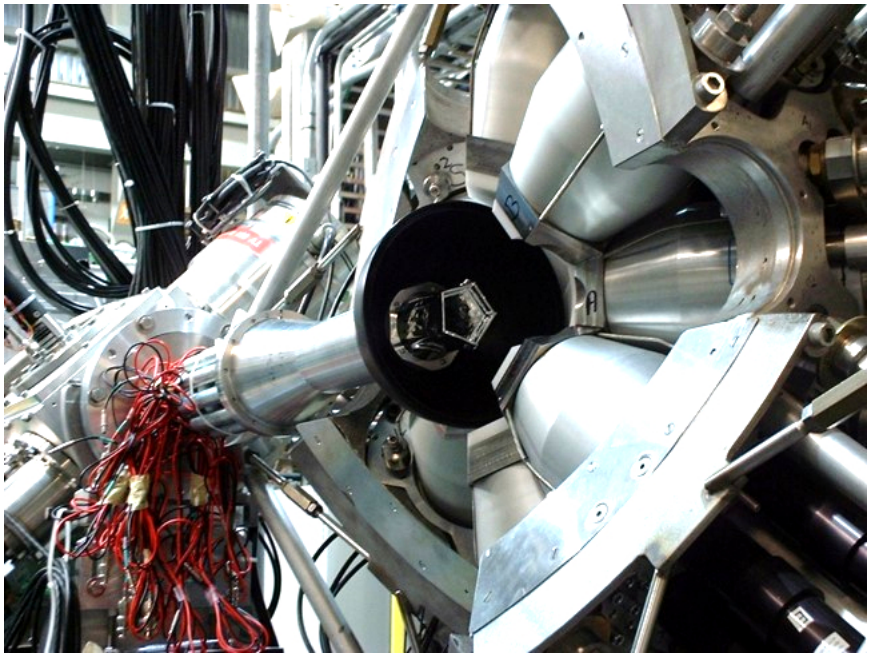

Figure 2. Photograph of one hemisphere of the 8π spectrometer surrounding one-half of the delrin vacuum chamber (black hemisphere in the center of the photograph). The plastic scintillator array SCEPTAR is seen inside the vacuum chamber. The vacuum chamber has an 9 cm outer radius.

will be followed by a description of the new GRIFFIN spectrometer that uses the same auxiliary detectors as the 8π spectrometer.

2. The 8π spectrometer

The 8π spectrometer and its associated detectors comprised four different detector systems; Compton-suppressed Ge detectors (the 8π Ge detector array) for γ-ray detection, plastic scintillators (named the SCintillating Electron Positron Tagging ARray – SCEPTAR) for detection of β particles, BaF_2 or $LaBr_3$ detectors (named the Di-pentagonal Array for Nuclear Timing Experiments – DANTE) for γ-ray detection with fast-timing capabilities, and Si(Li) detectors (named the Pentagonal Array for Conversion Electron Spectroscopy – PACES) for conversion electron studies. An integral part of the spectrometer was the Moving Tape Collector (MTC) and control over beam pulsing and tape cycling. Control of the MTC and beam pulsing, and readout of all detector systems, was performed by a data acquisition system that was optimized for both high throughput and high precision.

2.1. The 8π Ge detector array

The 8π spectrometer was composed of 20 high-purity Ge (HPGe) detectors equipped with Compton suppression shields of bismuth germanate (BGO) that formed an annulus around the Ge crystal as well as "back plugs" – small BGO crystals positioned behind the Ge crystals and surrounding the elongated shroud of the cold finger. Each Ge crystal possessed 20%–25% relative efficiency with respect to the standard 7.6 cm $\times$ 7.6 NaI crystals. The 20 individual HPGe detectors with their anti-Compton shields were arranged at the 20 hexagonal positions of a truncated icosahedron and occupy 4 rings of 5 detectors each at angles of $\pm 37^\circ$ and $\pm 79^\circ$ with respect to the beam direction. Figure 1 shows a photograph of one of the hemispheres of the 8π equipped with BaF_2 and $LaBr_3$ scintillators that were used for fast-timing applications. The source-to-front-face distance for the BGO suppression shields was $\approx$ 12.5 cm, and that for the Ge detectors was $\approx$ 14 cm. Collimators of 2.54 cm thickness made from densalloy were used to prevent the BGO shields and the outer radius of the coaxial Ge detectors from the direct irradiation from the source. Additional delrin shields with a thickness of 1.27 cm

covering the densalloy, and 3.81 cm covering the HPGe, could be installed (the white inner hemi-spherical shell in Fig. 1) that slows the high-energy β-particles that otherwise would reach the high-Z material – stopping most from entering the HPGe detectors – while minimising hard bremsstrahlung production due to its low effective Z. Figure 2 also shows one hemisphere of the 8π spectrometer, but with the upstream beam-line and one hemisphere of the vacuum chamber in place.

2.2. Beam pulsing and the MTC

One of the most important pieces of information garnered from β-decay studies is the half life of the decaying parent. Even in cases where this is known, measuring the apparent half life of the observed γ rays provides a very powerful method to confirm parentage since typically beams are a combination of isobars or molecular contaminants that must be discriminated against if they cannot be eliminated outright. In addition, in many studies of nuclei far from stability, the daughter nuclei are also radioactive, but often with half lives that increase as the valley of stability is approached. Thus, the activity inside the vacuum chamber can often increase with time beyond that of the original beam. In order to enable both half-life measurements and remove activity from the focal volume of the array, a moving tape collector and the ability to control the beam pulsing were incorporated into the spectrometer and its data acquisition system.

The moving tape collector uses a continuous loop of thin Al or Fe coated mylar tape up to a maximum length of $\approx$ 120 m. The entire tape system is held under vacuum, with the tape threaded through the downstream end of the beam line and through the center of the vacuum chamber. The tape, which is $\approx$ 13 mm in width and 50 μm thick, is kept under tension during its transit through the beam line and beam deposition position before being allowed to free fall into the evacuated, vertical, tape box. During tape movement, tape is pulled with a motor installed at the entrance of the tape box, and is extracted from the bottom of the box. The motor speed and duration of pull are controllable, although typical tape movements have a duration of 340 ms or 840 ms and pulls of 46 cm and 112 cm, respectively. In order to shield the downstream detectors from activity in the tape box, a Pb wall was built between the tape box and the 8π array. Figure 3 shows photographs of the tape placement in the vacuum chamber position in front of the downstream paddles of SCEPTAR (left), and the Zero-Degree Scintillator (ZDS) (middle), both of which are described below.

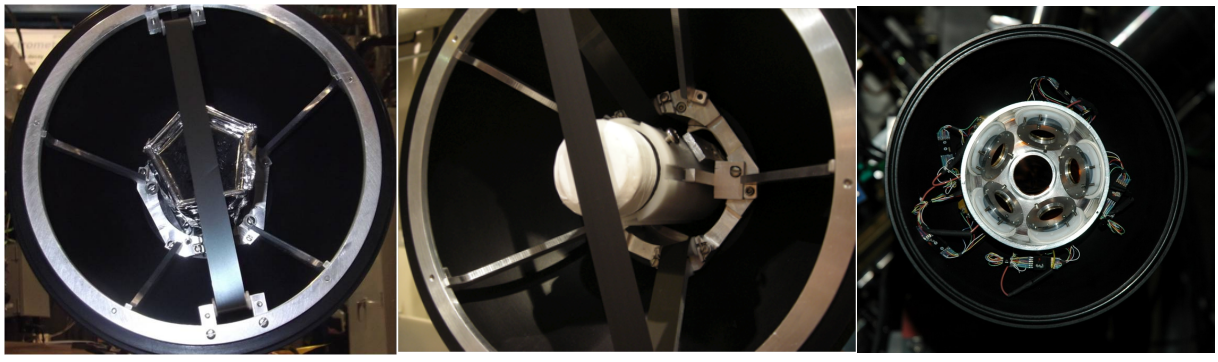

Figure 3. Photographs showing the detail of one half of the SCEPTAR array of plastic scintillators positioned on the downstream hemisphere behind the tape of the MTC (left), the ZDS behind the tape (center), and the PACES array of Si(Li) detectors (right) located on the upstream side of the vacuum chamber. PACES can be used in conjunction with either the SCEPTAR or ZDS detectors on the downstream side.

The beam pulsing can be controlled through the use of an electrostatic "kicker" placed in the ISAC beam line. A signal generated by a Jorway controller provided both the frequency and the dwell time of the beam, with a practical limit for the dwell time on the order of 10 ms.

2.3. SCEPTAR and the ZDS

Complementing the Ge detectors is the SCEPTAR array of 20 plastic scintillators that are arranged into 2 rings of 5 trapezoidal pieces and 2 rings of 5 rectangular pieces. The positioning is such that one plastic scintillator overlaps the solid angle of one Ge detector. The total solid angle coverage of SCEPTAR is approximately 80% of 4π. The plastic scintillators are BC404 of thickness 1.6 mm, located $\approx$ 4 cm from the beam implantation location. Each scintillator is wrapped in a thin aluminized mylar tape that acts as a diffuse reflecting surface. Light is collected from the edge of the scintillators and transported via $\approx$ 35 cm long lucite light-guides to the phototubes located outside of the main frame of the array. Figure 4 is a drawing showing the arrangement of one half of the SCEPTAR array in the hemisphere of the vacuum chamber, also visible in Fig. 2, and the light guides in the beam line. Due to the thinness of the BC404 scintillator, for many of the experiments SCEPTAR acts like a ΔE detector, with a slowly varying pulse height dependence on the β-particle energy. The β-particles with energy greater than $\approx$ 1 MeV pass through the detector and, for high β-particle energies ($>$ 3 MeV), deposit a nearly equal amount of energy (400 keV) in the plastic. While for many experiments the pulse height variation is of little consequence, for experiments aimed at studies of super-allowed Fermi decay, such a variation must be accounted for in the extraction of branching ratios. Measurements of the timing response of a SCEPTAR detector, performed by recording coincidences between one of the plastic scintillators and a BaF_2 detector, indicated a full width at half maximum (FWHM) in the range of 1–1.5 ns. A typical lower-energy threshold achieved was 30–40 keV.

For some experiments, it is desirable to use a plastic scintillator that has a faster time response, especially if used in timing applications, as well as a minimum of after-pulsing. To that end, the downstream half of the SCEPTAR array can be replaced with the ZDS. The ZDS is a 1 mm thick BC422Q scintillator coupled directly to a Hamamatsu H6533 photomultiplier assembly mounted inside the vacuum chamber. The ZDS is mounted on a rail that allows for movement from a position within a few mm to $\approx$ 5 cm behind the tape so that the count rate can be lowered to an acceptable level without decreasing the deposited beam activity. The maximum solid angle coverage is $\approx$ 25% of 4π.

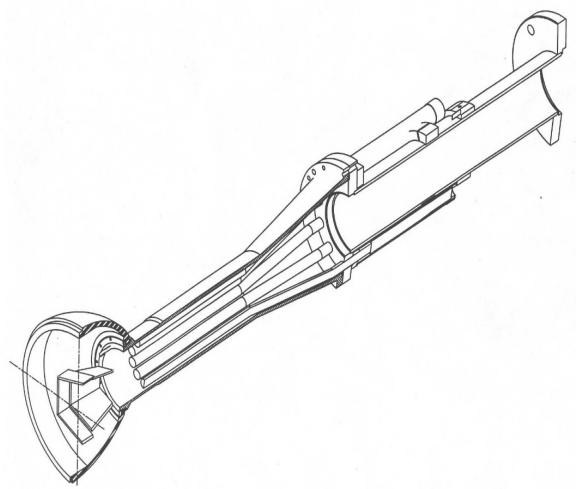

Figure 4. Drawing of one-half the SCEPTAR array in a hemisphere of the vacuum chamber (lower left). The light guides attach to the edges of the BC404 plastic and lay on the inside of the beam line until physically outside of the 8π array, a distance of $\approx$ 35 cm. The light guides are then coupled to the phototubes which reside outside of the beam line. In the drawing, for clarity the connection of the scintillator paddles to the light guides is not shown.

2.4. PACES

In order detect conversion electrons, an array of 5 Si(Li) detectors, PACES (Pentagonal Array for Conversion Electron Spectroscopy) can be installed. Inclusion of conversion-electron data provides not only multipolarity information, but also reveals electric monopole ($E0$) transitions indicative of shape coexistence effects. Further, in studies of nuclei with a large number of levels at low-excitation energy, as is often encountered in odd-odd nuclei or in the actinide region, the ability to detect low-energy conversion electrons and γ rays is vital in the construction of accurate decay schemes.

In order to install PACES, the upstream half of the SCEPTAR array is removed and the 5 Si(Li) detectors are installed. The 5 mm thick detectors, with a surface area of ≈ 250 mm^2, are located at a distance of 3 cm from the beam deposition position. The Si(Li) detectors are in thermal contact with an Al plate that is cooled by a annular Cu cold finger of 0.75 m length. The annular cold finger is placed inside the beam line, the annular opening allowing the beam to pass through. The Si(Li) detectors have a typical resolution of 2.5 keV at 1 MeV. A close-up view of the PACES array is shown in the right panel of Fig. 3. The available active area of PACES covers $\approx 5\%$ of 4π solid angle, making it an efficient device for coincidence studies.

2.5. DANTE

Using the available 10 open pentagonal positions in the frame of the 8π spectrometer (1 pentagon was used for the incoming beam line, and another for the vacuum system for the moving tape collector and SCEPTAR light guides), the 10 BaF_2 and $LaBr_3$ detectors of DANTE were installed. The BaF_2 scintillator is one of the fastest known; one of its two scintillating-light components has a decay constant of 0.6 ns and emits light in the UV region. The BaF_2 crystals were obtained from SCIONIX and are a monolithic piece in the shape of cylinder with a truncated cone atop. The truncated cone has 2 cm diameter at the top, 4 cm at the bottom, and 3 cm in length. The cylindical portion has a diameter 4 cm and 1.7 cm in length. The detectors are coupled to very fast photomultiplier tubes, the Photonis XP2020/URQ, having a quartz entrance window for maximum transmission of the fast-component UV light. The performance of the DANTE BaF_2 detectors was described in Ref. [7].

Since the BaF_2 detectors have energy resolutions of $\approx 8\%$, eight of them were replaced with 5.1 cm length $\times$ 5.1 cm diameter BrilLanCe(380) $LaBr_3$(Ce) detectors, obtained from St. Gobain. These detectors were designed to be placed within the BGO shields of the 8π array for their possible use with Compton suppression, although in practice this has not occurred. The $LaBr_3$ detectors have much improved energy resolution, on the order of 3%, while the timing resolution is practically unchanged from that of the BaF_2 detectors.

2.6. Data acquisition system

One of the prime goals of the 8π spectrometer was the performance of measurements of Fermi super-allowed β decay for CKM matrix unitarity tests. These measurements are extremely demanding, requiring half lives, branching ratios, and decay Q values measured (ideally) to better than 0.05% precision. This largely drove the form of the data acquisition system, requiring a high degree of diagnostics and accounting for every event generating a trigger. The other aspect for consideration was the desire to accumulate statistics as great as achievable within the fixed duration beam times, thus demanding a high throughput while at the same time possessing reliability. The approach adopted was to decouple the acquisition of data from the various detector subsystems described above. This was achieved by having, for each detector system, its own "data stream", with its own trigger and time stamping of all events, and readout to separate memory units. These data streams were then merged in software afterwards, and the appropriate correlations taken.

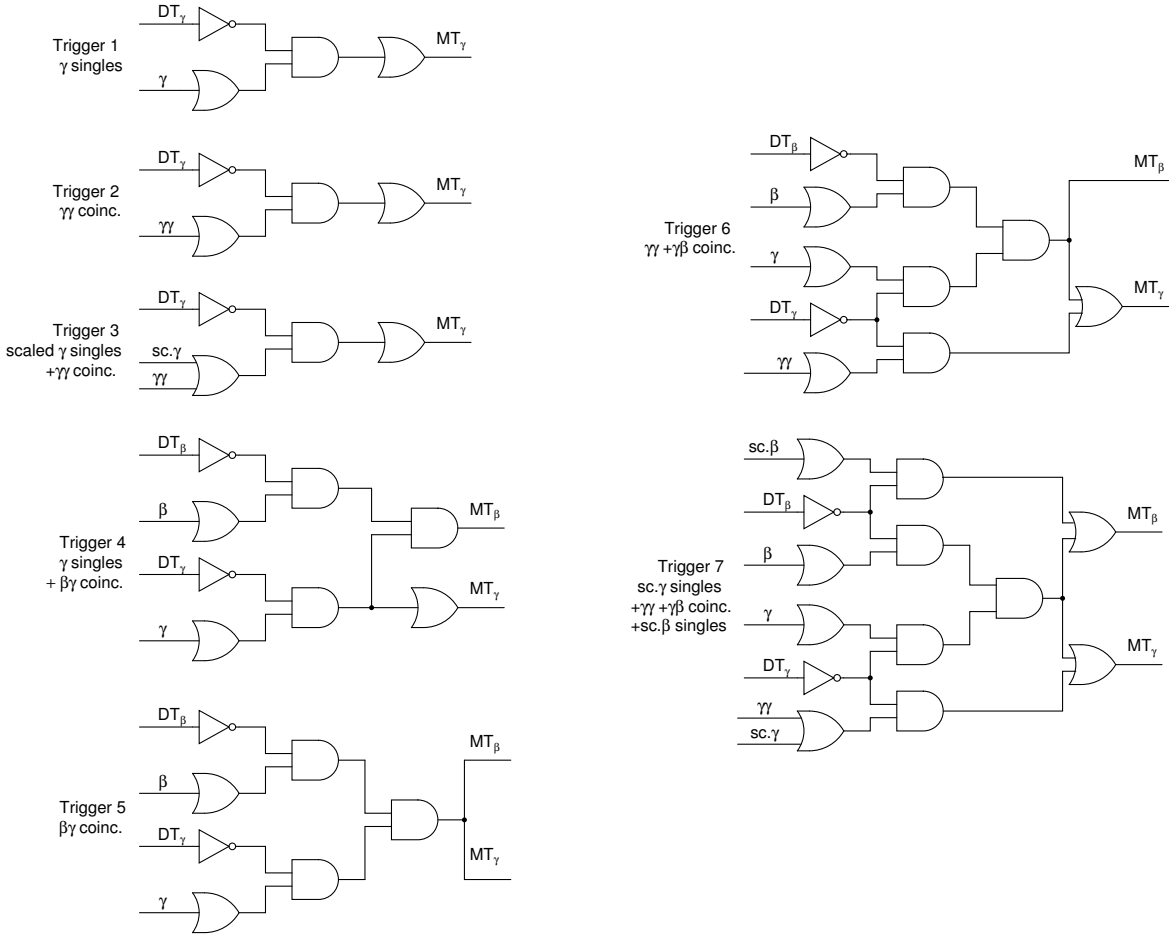

Figure 5. Examples of the trigger logic used in the 8π spectrometer for the first 7 programmed triggers. The nomenclature used is γ for the sum of all γ-ray singles signals, $\gamma\gamma$ for γ-γ-coincidences signals, derived from a LeCroy 4234 MALU (majority lookup unit) with a 1 μs coincidence window, β for the sum of all SCEPTAR singles events, sc for scaled-downed singles events, DT for the dead time signal, and MT for the master trigger that is delivered for each individual data stream. Each column of AND or OR gates represents a LeCroy 2365 octal logic unit, with the dead time NOT also routed via a separate 2365 octal logic. Only data streams that explicitly received a master trigger would process data. This arrangement provided a high-degree of flexibility, and 47 different trigger combinations were pre-programmed. The selection of the particular trigger was achieved at the beginning of an individual run via the entering of the trigger number on the data acquisition start-run interface.

While there are a number of data-acquisition standards that could have achieved the data-transfer rates necessary, the collaboration was already in possession of a large number of CAMAC modules, and in an effort to implement the most cost-effective system, it was decided to reuse as many of the these as possible. The FERA-based system, developed by LeCroy corporation in the 1980s, remains a very robust and highly-reliable data-acquisition standard, and is capable of high data-transfer rates of 200 ns per 16-bit data word, or 10 MB/s.

As the 8π spectrometer expanded in the number of detector sub-systems, the data

acquisition also expanded in its sophistication, eventually composed of 4 separate data streams corresponding to the four different detector types; Ge, SCEPTAR, DANTE, and PACES. Each data stream was triggerable separately, with its own independent dead time and readout. The triggering could involve single events, or coincidences both within and between the detector subsystems. The triggering was programmed with a series of LeCroy 2365 Octal Logic modules. Once a trigger for a particular detector system was generated, the appropriate gates were created for amplitude-to-digital converters (ORTEC single channel 14-bit AD114s or 4-channel 13-bit AD413As), and STOP signals for time-to-digital converters (LeCroy 3377 Multi-Hit TDCs). Time stamps for the events in each data stream were generated by counting a precision 10 MHz pulser in LeCroy 2366 or 2367 universal logic modules (ULM) programmed to act as latching scalers, with the latching provided by the trigger signals. The data streams were controlled by CMC203 FERA drivers, with data passed to Struck SIS3700 32-bit ECL FIFO memory units located in a VME crate.

In the offline sorting, events were first correlated with the time stamps of the ULMs, followed by the data from the TDCs. Since the ULMs were latched by the trigger signal, which was also used as the STOP signal for the TDCs, by taking the appropriate combination of data the event times with respect the the beginning of the particular cycle could be generated, as well as the event times between any two detectors independent of the time of the trigger. This was particularly important for situations that often arose where one detector stream was triggered on singles events, with the trigger for a different data stream generated only upon a coincidence. In addition to the event times, the dead times on an event-by-event basis were also recorded by counting the 10 MHz clock pulses vetoed by a pulse of duration of the dead time. The precision and accuracy of the system was tested with a ^{26}Na decay experiment, where the half life was well determined by β-particle counting [4]. The system proved capable of measuring half lives by gating on photopeaks on the Ge detector spectra accurate to within a precision of 0.05%, provided that an accurate determination of the effects of pulse pile-up were taken into account [5]. In addition, the plastic scintillator detectors of SCEPTAR were also used to measure half lives, requiring a determination of the after-pulsing of the scintillator to be taken into account [6].

3. Spectroscopy of ^{124}Xe and the nature of the low-lying 0^+ bands

The investigation of the decay of ^{124}Cs to ^{124}Xe is part of a wider programme of study of the nature of collectivity and how it evolves in nuclei. While there has been a great deal of attention paid recently to regions of the nuclear chart where there are rapid changes in structure, the region "north-west" of ^{132}Sn displays a remarkably smooth evolution of its excitation energy spectrum, as evinced by the 2^+_1 energies and described in Ref. [8].

Recent Coulomb excitation studies [9, 10, 12, 13] have been performed using Xe beams bombarding a ^{12}C target with the de-excitation γ rays detected with the GAMMASPHERE array. These studies have resulted in a large set of transition matrix elements where the populations of the states were dominated by single-step transitions from the ground state. Included in the set of matrix elements were those for transitions from 2^+ band members of excited "$K^\pi = 0^+$" bands, specifically for the 0^+_2 band and the conjectured 2^+ member of the 0^+_3 band. These $2^+ \rightarrow 0^+$ in-band matrix elements possessed very large uncertainties since they were not directly observed, but their magnitudes were ascertained from the yields observed for the out-of-band transitions from the 2^+ states. The $2^+_3 \rightarrow 0^+_2$ $B(E2)$ value was deduced to be 62 ± 36 W.u., with the $B(E2; 2^+_4 \rightarrow 0^+_3)$ value in the range of 5–68 W.u. [9].

Since the low-energy, in-band transitions are expected to be very weak, with branching ratios of a few percent or less, γ-ray detection following β decay offers the most promising technique that would allow their observation. An experimental programme was launched in 2011 with the goal of studying the β decay of the even-mass Cs isotopes, with ^{124}Cs being the first decay

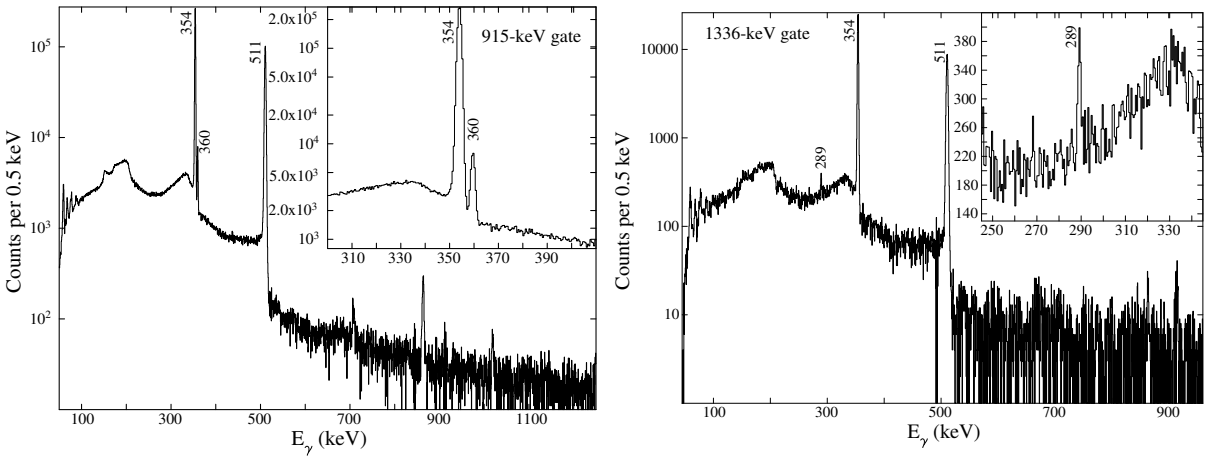

Figure 6. Portions of the γ-ray coincidence spectra gated on the 915-keV $0_2^+ \rightarrow 2_1^+$ γ ray showing the 360-keV γ ray from the 1629-keV level (left), and the 1336-keV $0_3^+ \rightarrow 2_1^+$ γ ray showing the 289-keV γ ray from the 1979-keV level (right). The insets display expanded regions of the spectra to show the γ rays of interest in more detail. The intensity of the 289-keV γ is approximately 10^{-5} that of the 354-keV $2_1^+ \rightarrow 0_{gs}^+$ γ ray. From Ref. [14].

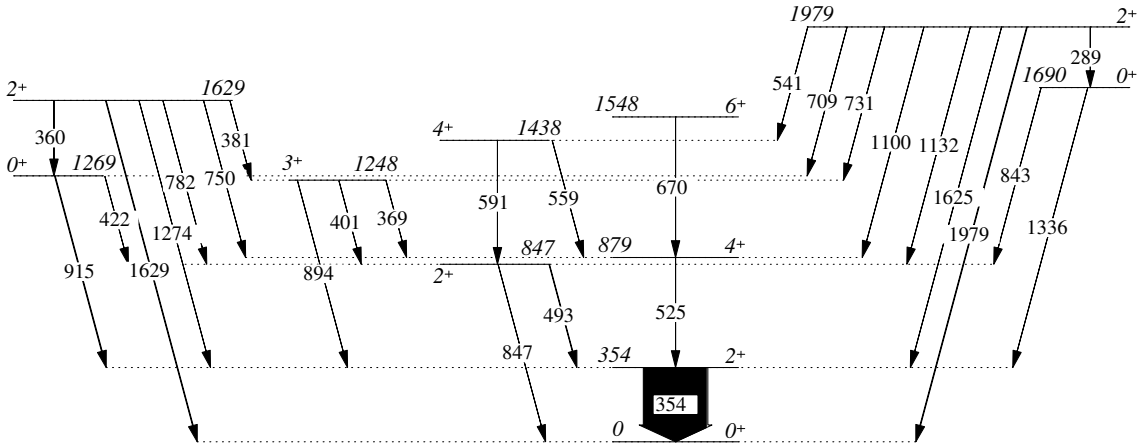

Figure 7. Partial level scheme of ^{124}Xe observed in the β^+/EC-decay of ^{124}Cs. Levels are labelled with their energies in keV, and their J^π values. The transitions are labelled with their energies in keV, with arrow widths proportional to the observed intensity. From Ref. [14].

measured. A beam containing 9.8×10^7 ions/s ^{124}Cs ($J^\pi = 1^+$, $T_{1/2} = 30.8$ s) and 2.6×10^6 ions/s ^{124}Cs^m ($J^\pi = (7)^+$, $T_{1/2} = 6.3$ s) resulted from the bombardment of a ^{nat}Ta target with 25 μA of 500 MeV protons from the TRIUMF main cyclotron. The beam was deposited on the tape at the center of the 8π array with scaled-downed γ-ray single events and γ-γ coincidence data collected during the implantation and decay period. The cycle times for the beam deposition and tape movement varied from short implantation and decay times to optimize the data for decay of the high-spin isomer, to much longer times to optimize the statistics for decay of the longer-lived low-spin ground state. For the long-cycle times, the data were sorted into a time-random-background subtracted γ-γ coincidence matrix containing approximately 4.5×10^8 events.

The full analysis of the γ-γ coincidence data has resulted in a decay scheme with several hundred transitions and over a hundred levels, but here only the in-band $2^+ \rightarrow 0^+$ transitions in the 0_2^+ and 0_3^+ bands will be discussed. The left panel of Fig. 6 displays a portion of the spectrum resulting from a coincidence gate on the 915-keV $0_2^+ \rightarrow 2_1^+$ γ ray – the dominant decay branch from the 0_2^+ band head. The partial level scheme highlighting the $K^\pi = 0^+$ bands is shown in Fig. 7. The measured [14] branching ratios for the 360-keV $2_3^+ \rightarrow 0_2^+$ and 289-keV $2_4^+ \rightarrow 0_3^+$ transitions were 5.81(27)% and 0.79(9)%, respectively, resulting in $B(E2; 2^+ \rightarrow 0^+)$ values of 78(13) W.u. and 53(12) W.u., where the $2^+ \rightarrow 0_{gs}^+$ $B(E2)$ values were taken from the Coulomb excitation analysis [9] and used as the reference transition. Figure 6 demonstrates the importance of high-resolution measurements that enable the observation of the 360-keV γ ray located near the much stronger 354-keV $2_1^+ \rightarrow 0_{gs}^+$ γ ray, and high-sensitivity achieved due to the Compton suppression that enabled the observation of the 289-keV γ ray in the presence of large backgrounds from Compton scattering of other γ rays.

The present data demonstrates the power of combining complementary techniques; since the Coulomb excitation matrix elements were already available, the measurement of new branching ratios immediately provides new $B(E2)$ values. (New calculations of the Coulomb excitation yields verified that their change due to the new branching ratios were not significant.) The set of $B(E2)$ values now available and precisely determined enables the use of the Kumar-Cline sum rules [15] for the 0^+ states – an analysis that could not be undertaken previously. For the 0^+ states, the rotationally-invariant $E2$ moments can be found using

$$\frac{1}{\sqrt{5}}Q^2 = \sum_i \langle 0\|\mathcal{M}(E2)\|2_i\rangle\langle 2_i\|\mathcal{M}(E2)\|0\rangle \begin{Bmatrix} 2 & 2 & 0 \\ 0 & 0 & 2 \end{Bmatrix} \tag{1}$$

where $\mathcal{M}(E2)$ is the transition matrix element and $\{\}$ is a $6j$ symbol. The Q^2 invariant can be related to the β_0 shape parameter within the axially-symmetric rotational model via

$$Q^2 = q_0^2\beta_0^2 \tag{2}$$

with $q_0 = \frac{3}{4\pi}ZR_0^2$ with $R_0 = 1.2A^{\frac{1}{3}}$ fm. The values of β_0 determined using the present data are given in Fig. 8 together with the values predicted by the IBM [9] and DPPQ model [16]. In principle, the experimental values represent lower limits, but are unlikely to change significantly

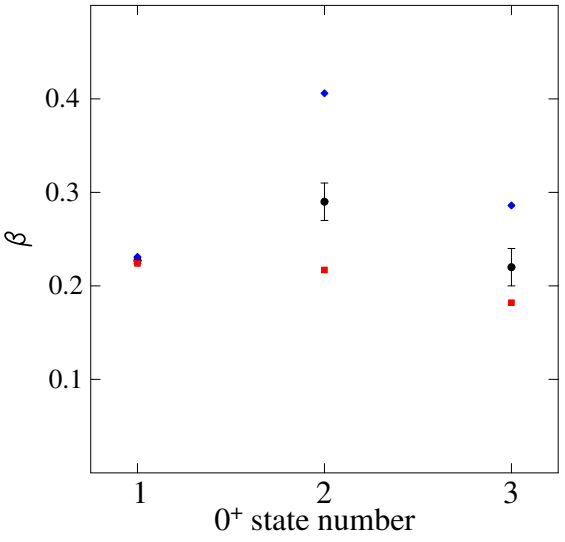

Figure 8. Magnitudes of the deformation parameter β_0 determined from Eqs. 1 and 2 for the 0_1^+ (ground state), 0_2^+ and 0_3^+ states [14]. The experimental values are black circles shown with error bars; the values from the interacting boson model calculation of Ref. [9] as red squares, and those from the dynamic pairing plus quadrupole model of Ref. [16] are blue diamonds. The agreement for the ground state is a result of the models fitting the $B(E2; 2_1^+ \rightarrow 0_{gs}^+)$ value.

by extending the sum over more states. Since models typically fit the $B(E2; 2_1^+ \rightarrow 0_{gs}^+)$ values, the agreement for the ground state is not significant.

The apparent quadrupole collectivity of the 0_3^+ state, as measured by its β_0 value, does not suggest any special character beyond what collective models normally predict. However, the results of (^{3}He,n) reactions on the stable Te isotopes [17] revealed strong populations of the 0_3^+ levels in $^{124-130}$Xe, on the order of 35–40% of the ground state cross sections, indicating collective excitations of the pairing type. In nuclei near closed shells, such strong transitions are a signature of pairing vibrations (see, e.g. Ref [18]), and thus the 0_3^+ levels in these Xe isotopes must have the main fragments of the proton 2-phonon pairing vibration [14]. Pairing vibrations are outside the normal IBM model space, and thus the 0_3^+ level cannot be associated with the $\sigma = N - 2$ state as in Ref. [9]. This result emphasizes the need for comprehensive spectroscopy using many different probes in making structural assignments.

4. Internal decay of ^{124}Cs^m

In addition to the decay of the ^{124}Cs ground state, the decay of ^{124}Cs^m that was present in the beam was also observed. The transitions originating from this decay, which has a half life of 6 s, were enhanced in the data obtained with the short tape cycles. The study of the internal decay of the ^{124}Cs^m state could only be completed with the use of the PACES array for detection of conversion electrons. Shown in the left-hand panel of Fig. 9 is a typical Si(Li)-detector spectrum obtained with a coincidence gate on the 189-keV γ ray that is in the decay path of the ^{124}Cs (7^+) isomer. Using the γ-e^- coincidence data, together with γ-γ coincidence data, the decay

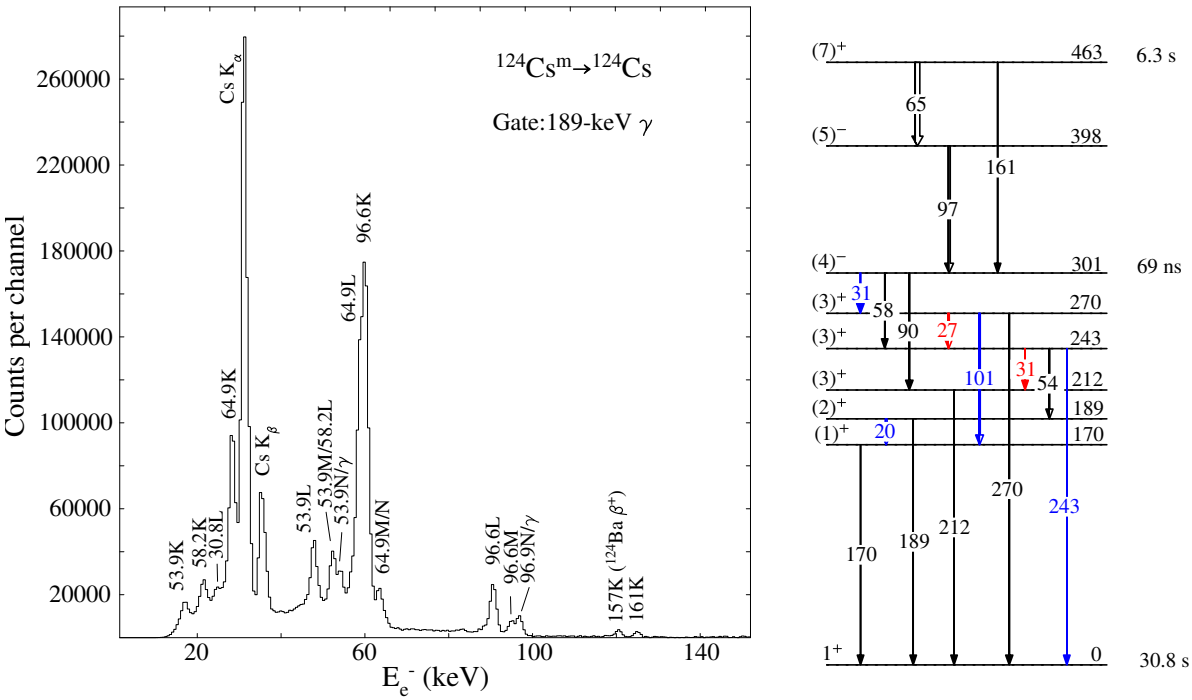

Figure 9. Portion of the γ-e^- coincidence spectra gated on the 189-keV $2^+ \rightarrow 1_{gs}^+$ γ ray (left) in ^{124}Cs. The peaks are labelled with the transition of origin. Level scheme (right) deduced for the isomeric decay of ^{124}Cs^m. Levels are labelled with their energies in keV, and their J^π values. The transitions are labelled with their energies in keV, with arrow widths proportional to the observed intensity and white-filled arrows showing the degree of conversion. Arrows in blue are previously unobserved transitions in the decay of the isomer, with those in red new transitions.

scheme as shown in the right-hand panel of Fig. 9 was constructed.

5. The transition to GRIFFIN

While the 8π spectrometer was very successful and was the world's most sensitive γ-ray spectrometer dedicated to β-decay studies, the improvement in Ge detector technology over the past 30 years made an obvious case to replace the 8π with a new spectrometer. It was deemed that the geometry employed for TIGRESS [19], that of a rhombicuboctahedron, offered the optimum design with a compromise in solid angle coverage, number of individual HPGe detectors, angle combinations for angular correlation measurements, and flexibility for accommodating auxiliary detectors. The Gamma-Ray Infrastructure For Fundamental Investigations of Nuclei (GRIFFIN) consists of up to 16 large-volume n-type HPGe detectors of the clover design, with each HPGe crystal of the clover possessing an average 41% relative intrinsic efficiency. Operated in add-back mode, each of the clover detectors of GRIFFIN is equivalent to a single HPGe with $\approx$ 220% relative efficiency. The crystals of the GRIFFIN clover detectors also possess outstanding energy resolution, averaging 1.1 keV at 121 keV, and 1.9 keV at 1332 keV.

In order to have as smooth a transition as possible from the 8π array to GRIFFIN, the same vacuum chamber was adopted, and GRIFFIN was designed so that the HPGe detectors (with their planned future BGO Compton suppression shields) to have close-packing with an 11 cm inner radius. GRIFFIN, when completed with Compton suppression shields, will have two standard operating modes; a "maximum efficiency" mode with the front faces of the HPGe detectors at 11 cm and the BGO front shield retracted, and a "optimized peak-to-total" mode with the HPGe detector front faces at 14.5 cm and the BGO front shields moved forward to provide maximum coverage and collimation of the Ge crystals. As shown in Fig. 10, which displays calculated photopeak efficiencies using the GEANT4 simulation package, GRIFFIN provides an enormous boost in single γ-ray detection efficiency over the former 8π spectrometer, whether considering the 64 single Ge crystals, taking advantage of the crystal arrangement and applying add-back within the clover detector, or using adjacent clover detectors in the add-back scheme. Panel a) on the left of Fig. 10 shows that single γ-ray efficiencies as high as 25% at 1 MeV can be achieved.

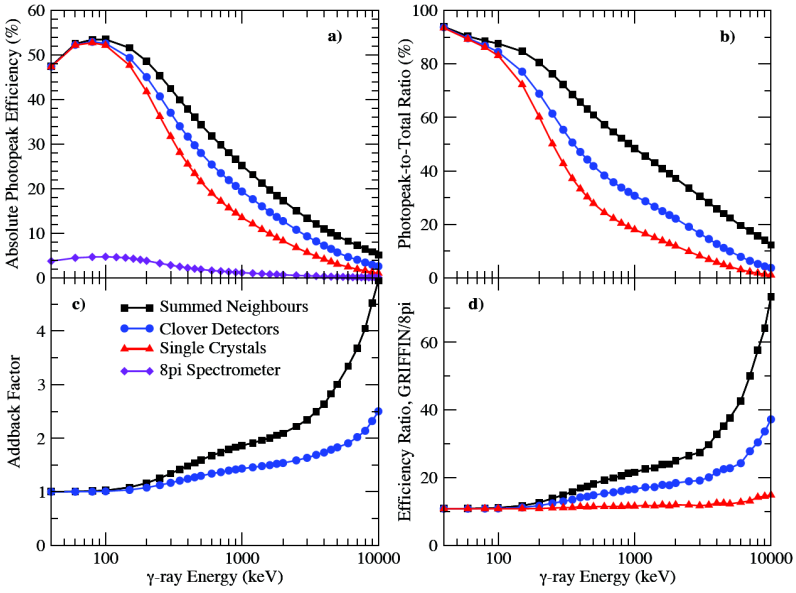

Figure 10. Simulations of the performance of the GRIFFIN and 8π spectrometers using the **GEANT4** code. The simulations were performed assuming a single γ ray interacting with the array with the energy as given by the abscissa. Panel a) shows the photopeak efficiency, panel b) the peak-to-total ratio, panel c) the ratio of the efficiency with:without add-back, and panel d) the ratio of the efficiency with respect to the 8π spectrometer.

The increased GRIFFIN γ-ray detection efficiency enables experiments to be performed that were marginal with the 8π spectrometer, especially when considering the need for γ-γ coincidences where the coincidence rate increases approximately with the square of the efficiency. However, as many experiments with the 8π spectrometer were count-rate limited rather than efficiency limited, an early decision was made to develop a data acquisition system that could provide at least an order of magnitude improvement in the data through-put over the 8π spectrometer. The goal set for the design of the GRIFFIN data acquisition system is to enable a sustained rate of 300 MB/s of data to disk – sufficient to allow the single GRIFFIN Ge crystals to run at 50 kHz rates.

A custom-built fully-digital data acquisition system, residing in VME, has been designed and constructed for GRIFFIN. The heart of the system rests on two front-end digitizers; a 14-bit 100 MHz 16-channel module labelled as GRIF-16, and a 12-bit 1 GHz 4-channel module, the GRIF-4G. The GRIF-16 processes signals from detectors where high-spectroscopic quality is needed, such as the Si(Li) or HPGe detectors, whereas the GRIF-4G processes the much-faster signals from SCEPTAR or DESCANT detectors. The data from the front-end modules is passed to two levels of collector modules, the GRIF-C, via a 625 MB/s link to each digitizer. The GRIF-C is designed to accommodate 1.25 GB/s data transfer rate at peak. The lower-level GRIF-C passes its data to a master collector GRIF-C module that can run a filter algorithm to determine which data are written to disk. All modules are synchronized via the GRIFFIN clock (GRIF-CLK) that uses a single 10 MHz atomic clock signal in the Master Clock that is distributed and fanned-out via slave GRIF-CLK modules to the rest of the system modules. The NIM or TTL signals for the moving tape collector, the beam kicker, and other potential devices requiring slow control are generated via a programmable pulse generator, the GRIF-PPG, that is controlled by the GRIF-C Master.

Following the dismantling of the 8π spectrometer in January 2014, the installation of GRIFFIN commenced with the commissioning experiment in September 2014 to study the decay of ^{115}Ag. Figure 11 is a photograph of one hemisphere of GRIFFIN showing 7 of the GRIFFIN HPGe detectors supplemented by one TIGRESS detector with its BGO side shield. The photograph shows the "maximum efficiency" mode with the detectors positioned fully

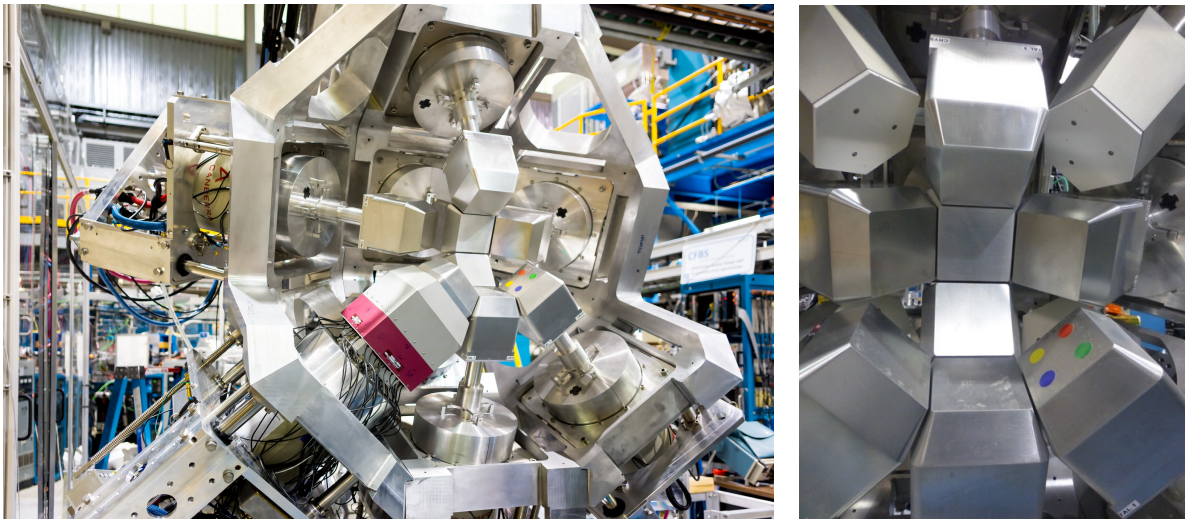

Figure 11. Photograph (left) of one hemisphere of the GRIFFIN spectrometer configured for the commissioning experiment on ^{115}Ag decay, September 2014. The photograph on the right shows detail of the configuration of the GRIFFIN spectrometer for the study of ^{32}Na decay where it is supplemented with DESCANT detectors in the open triangular positions of the frame.

forward at 11 cm from the beam deposition point. Also visible in Fig. 11 are large circular openings in the triangular sections of the array for potential supplementation with auxiliary detectors. Such an arrangement is shown in the right panel of Fig. 11 where the DESCANT detectors [20] for neutron detection were used to study the decay of ^{32}Na.

The study of the decay of ^{32}Na, performed in late November, 2014, is under analysis and the preliminary results indicate that GRIFFIN performs as predicted. Compared with an earlier experiment with the 8π spectrometer [21], which was performed for a duration of 5 days with 2–3 ions/s of ^{32}Na, the new GRIFFIN experiment had a duration of only 2 days with a beam rate of approximately 9 ions/s. The results of γ-γ coincidence gating indicate more than 2 orders of magnitude increase in statistics. This level of statistics is sufficient for an angular correlation analysis on the stronger transitions, enabling spin-parity assignments of the excited states.

6. Conclusions

The 8π spectrometer proved to be an enormous asset for the TRIUMF-ISAC facility, and despite the obvious obsolescence in its Ge-detector technology, due to its dedicated nature it was proven to be the most sensitive γ-ray spectrometer used for β-decay studies. Continuous improvements in the auxiliary detectors, the data acquisition, and influx of new ideas helped to keep the 8π on the forefront of nuclear structure physics, and although not addressed in the present work, its contributions to superallowed Fermi β-decay studies are nearly unparalleled.

Despite its successes, a replacement of the 8π spectrometer was required to keep γ-ray spectroscopy at TRIUMF-ISAC at the forefront, especially in consideration of improvements in the ISAC facility and the development of the ARIEL [22]. The GRIFFIN spectrometer, representing at least two-orders-of-magnitude improvement in sensitivity of γ-γ coincidences heralds a new era that will enable detailed spectroscopic studies not only of nuclei near stability, but also far from stability.

Acknowledgments

This work was supported in part by the Natural Sciences and Engineering Research Council (Canada), TRIUMF through the National Research Council (Canada), and by the U.S. National Science Foundation under Grant No. PHY-1305801. Funding for GRIFFIN was provided by the Canadian Foundation for Innovation, TRIUMF, and the University of Guelph.

References

[1] Garrett PE *et al.* 2007 *Nucl. Instrum. Meth.* **B261** 1084
[2] Garnsworthy AB and Garrett PE 2014 *Hyper. Int.* **225** 121
[3] Svensson CE and Garnsworthy AB 2014 *Hyper. Int.* **225** 127
[4] Grinyer GF *et al.* 2005 *Phys. Rev. C* **71** 044309
[5] Grinyer GF *et al.* 2007 *Nucl. Instrum. Meth.* **A579** 1005
[6] Triambak S *et al.* 2012 *Phys. Rev. Lett.* **109** 042301
[7] Cross DS *et al.* 2011 *J. Instrum.* **6** P08008
[8] Rowe DJ and Wood JL 2010 *Fundamentals of Nuclear Models: Foundational Models* (World Scientific, Singapore)
[9] Rainovski G *et al.* 2010 *Phys. Lett.* **B683** 11
[10] Coquard L *et al.*, *Phys. Rev. C* **83** 044318
[11] Heyde K and Wood JL 2011 *Rev. Mod. Phys.* **83** 1467
[12] Coquard L *et al.* 2009 *Phys. Rev. C* **80** 061304(R)
[13] Coquard L *et al.* 2010 *Phys. Rev. C* **82** 024317
[14] Radich AJ *et al.* 2015 *Phys. Rev. C* **91** 044320
[15] Cline D 1986 *Ann. Rev. Nucl. Part. Sci.* **36** 683
[16] Gupta JB 2014 *Nucl. Phys.* **A927** 53
[17] Alford WP *et al.* 1979 *Nucl. Phys.* **A323** 339
[18] Bohr A and Mottleson BR 1975 *Nuclear Structure* (W. A. Benjamin, Inc., Reading, Massachusetts)

[19] Hackman G and Svensson CE 2014 *Hyper. Int.* **225** 241
[20] Garrett PE 2014 *Hyper. Int.* **225** 137
[21] Mattoon CM *et al.* 2007 *Phys. Rev. C* **75** 017302
[22] Dilling J, Krücken R, Merminga L, 2014 *Hyp. Interact.* **225** 253